AIAA 81-1586R

Stagnation Point Combustion of a Monopropellant

G. Adomeit*
Rheinisch-Westfälische Technische Hochschule, Aachen, Federal Republic of Germany
and
W. Hocks†
Bayer AG, Leverkusen, Federal Republic of Germany

The steady-state stagnation point transport and reaction equations describing premixed monopropellant combustion have been investigated approximating the chemical processes by an endothermic solid-phase pyrolysis and a one-step exothermic unidirectional gas-phase reaction. The solution giving essentially the burning rate dependence upon external parameters was obtained for the limiting cases of frozen and equilibrium flow in closed form. The general case was treated numerically. It is found that the burning rate in the whole range depends upon the velocity U and the temperature T_e of the freestream flow. This dependence is particularly strong in the vicinity of the ignition and quench limits. For low flow velocities the burning rate becomes equal to the strand burning value. For high flow velocities the influence of the gas-phase reaction drops out. Then the burning rate is determined by the rate of the pyrolysis only. It may lie above or below the strand burning value. From these results steady-state ignition and quench limits can also be obtained. The numerical results have been obtained for ammonium perchlorate data. The conclusions drawn are valid, however, as long as the general physical model chosen applies.

Nomenclature

a = velocity gradient du_e/dx
A_i, B_i = molecular species
b = linear burning rate
B = frequency factor of the gas-phase reaction
B_s = frequency factor of the pyrolysis reaction
c_p = mean specific heat capacity of gas at constant pressure
c_{ps} = mean specific heat capacity of solid
E = activation energy of the gas-phase reaction
E_s = activation energy of the solid-phase reaction
f = nondimensional stream function, $f_\eta = u/u_e$
h = specific enthalpy
h^0 = enthalpy of formation
Δh_s = enthalpy of pyrolysis
ΔH_s = nondimensional enthalpy of pyrolysis, $\Delta H_s = \Delta h_s / c_p T_r$
j_i = diffusion mass flux
J_i = nondimensional diffusion mass flux, $j_i/\sqrt{(\rho\mu)_r a} = -(\ell Le_i/Pr)\,dY_i/d\eta$
ℓ = Chapman-Rubesin parameter $\ell = (\rho\mu)/(\rho\mu)_r$
Le_i = Lewis number of species i
$\dot{m}$ = burning rate
$\dot{M}$ = nondimensional burning rate, $\dot{M} = \dot{m}/2\sqrt{(\rho\mu)_r a}$
$\bar{M}_i$ = molecular weight of species i
n, m = temperature exponents in the rate law
p = pressure
Pr = Prandtl number
r = rate of gas-phase reaction
R = universal gas constant
R_D = ratio of Damköhler numbers
T = absolute temperature
u = tangential flow velocity
U = freestream velocity
v = normal flow velocity
V = nondimensonal normal velocity, $V = \rho v/2\sqrt{(\rho\mu)_r a}$
w_i = mass rate of production of species i in the gas phase
W_i = nondimensional mass rate of production of species i in the gas phase, $= w_i/a\rho$
x = tangential coordinate
y = normal coordinate
Y_i = mass fraction of species i
$\bar{Y}_i$ = relative mass fraction
η = nondimensional boundary-layer coordinate, $d\eta = \sqrt{a/(\rho\mu)_r}\rho dy$
μ = coefficient of viscosity
ν_i = stoichiometric coefficient
ϑ = coupling function
θ = nondimensional temperature, T/T_r
ρ = density

Subscripts

e = edge of boundary layer
f = flame ($a \to 0$)
i = ignition
j = species j
o = quiescent
r = reference
s = solid
u = inside solid ($\eta = -\infty$)
w = surface
η = differentiation with respect to η

Introduction

IT is well known from rocket propulsion that the burning rate of a composite propellant depends upon the flow velocity of the gas passing over the propellant surface. This effect has been investigated widely and is generally attributed to turbulence.[1,2] However, a dependence of this kind is also present for monopropellants in laminar flow, as is suggested by the influence of the Reynolds number upon ignition delay times,[3,4] but it has been investigated to a much less satisfactory degree.[5,6] As a consequence of this state-of-the-art either experimental rate data obtained under constant volume conditions are used or results derived for composite

Presented as Paper 81-1586 at the AIAA/SAE/ASME 17th Joint Propulsion Conference, Colorado Springs, Colo., July 27-29, 1981; submitted Sept. 1, 1981; revision received Feb. 16, 1982.

*Professor. Member AIAA.
†Chemical Engineer.

propellants are applied to monopropellant systems for which the influence of the flow velocities is to be accounted.[7] Furthermore, the concept of a constant ignition temperature is used widely when computing monopropellant ignition processes.[7]

To elucidate this problem the steady-state transport and reaction equations for stagnation-point flow are investigated. The chemical reactions are approximated by a two-step process consisting of an endothermic pyrolysis at the surface and a one-step exothermic unidirectional gas-phase reaction, the rates for both of which are described by an Arrhenius law. Radiative losses are neglected and inside the solid only heat conduction is taken into account. For the two limiting cases of frozen and equilibrium flow, the gas-phase reaction drops out and a closed-form solution is derived which relates the burning rate to the conditions at the propellant surface and in the freestream flow.

In the general case the nonlinear stiff second-order boundary value problem is treated as an initial value problem and solved numerically by a shooting method using the EPISODE package of Byrne and Hindmarsh.[8] The computations were carried out using the thermophysical data given by Johnson and Nachbar[9] for ammonium perchlorate (Ref. 9, Table 1, col. 2). The conclusions drawn from these results are valid, however, as long as the physical model chosen is applicable.

Balance Equations

The geometrical configuration investigated is shown in Fig. 1. A monopropellant surface is blown at with an inert gas having the temperature T_e and the velocity v_e at the edge of the boundary layer. The monopropellant pyrolyses give the gaseous reactants A_i which may, in turn, react in the gas phase to form the products B_i. The stagnation-point region is considered.

The balance equations for this axisymmetric stagnation point boundary-layer flow are[10,11]

Mass:

$$\frac{\mathrm{d}V}{\mathrm{d}\eta}+f_\eta=0 \tag{1}$$

Momentum:

$$2Vf_{\eta\eta}-(\ell f_{\eta\eta})_\eta-(\rho_e/\rho-f_\eta^2)=0 \tag{2}$$

Energy:

$$2V\theta_\eta-\frac{1}{c_p}\left(\frac{c_p\ell}{Pr}\theta_\eta\right)_\eta+\sum_{i=1}^{N}(c_{pi}/c_p)J_i\theta_\eta+\sum_{i=1}^{N}W_ih_i/c_pT_r=0 \tag{3}$$

Species i:

$$2VY_{i\eta}+J_{i\eta}-W_i=0 \tag{4}$$

where the nondimensional diffusion mass flux is, in the binary mixture approximation,

$$J_i=j_i/\sqrt{(\rho\mu)_r a}=-\ell(Le_i/Pr)\,\mathrm{d}Y_i/\mathrm{d}\eta \tag{5}$$

In Eq. (3) dissipative effects have been neglected.

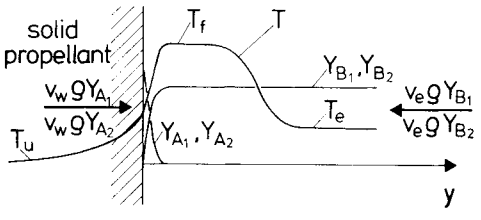

Fig. 1 Stagnation point region of monopropellant surface burning in inert gas crossflow.

The boundary conditions are

$$\eta=0:\quad f_\eta=0,\quad -f=V_w=\dot{M}=\dot{m}/2\sqrt{(\rho\mu)_r a}$$

$$\frac{\mathrm{d}\theta}{\mathrm{d}\eta}=2\frac{Pr}{\ell}\dot{M}\left[\Delta H_s+\frac{c_{ps}}{c_p}(\theta_w-\theta_u)\right],\quad J_i+2\dot{M}Y_i=\dot{M}_i \tag{6}$$

$$\eta\to\infty:\quad f_\eta=u/u_e=1,\quad \theta=\theta_e,\quad Y_i=Y_{ie} \tag{7}$$

Assuming the gas-phase reaction to be a one-step, unidirectional reaction,

$$\sum_{i=1}^{N}\nu_i' A_i\to\sum_{i=1}^{N}\nu_i'' B_i \tag{8}$$

with

$$\nu_i=\nu_i''-\nu_i'$$

the mass rate of production of species i is

$$w_i=\bar{M}_i\nu_i r \tag{9}$$

where r is the rate of the gas-phase reaction

$$r=B\prod_{j=1}^{N}\left(\frac{\rho Y_j}{M_j}\right)^{\nu_j'}T^n\exp(-E/RT) \tag{10}$$

The solid-phase pyrolysis reaction is assumed to proceed via the reaction

$$\text{solid}\to\sum_{i=1}^{N}\nu_i' A_i \tag{11}$$

with the mass rate of production

$$\dot{m}=\rho_s B_s T_w^m\exp(-E/RT_w) \tag{12}$$

Transformed Boundary-Layer Equations

These equations may be transformed to allow the introduction of a coupling function $\vartheta(\eta)$ and also to make use of constants introduced by Johnson and Nachbar.[9]

Introducing

$$Y_i'=\frac{\nu_i'\bar{M}_i}{\Sigma\nu_i'\bar{M}_i},\qquad Y_i''=\frac{\nu_i''\bar{M}_i}{\Sigma\nu_i''\bar{M}_i} \tag{13}$$

a relative mass fraction

$$\bar{Y}_i=(Y_i-Y_i')/(Y_i''-Y_i') \tag{14}$$

may be defined. Substituting this quantity in Eqs. (1-7), assuming $c_p=c_{pi}=\text{const}$ and $Le_i=1$, setting

$$c_pT_r=-\frac{\Sigma\bar{M}_i\nu_i h_i^0}{\Sigma\nu_i'\bar{M}_i} \tag{15}$$

and replacing the velocity gradient a in the nondimensional reaction rate term by $\dot{M}$, we obtain

$$\frac{\partial V}{\partial\eta}+f_\eta=0 \tag{16a}$$

$$2Vf_{\eta\eta}-(\ell f_{\eta\eta})_\eta-(\rho_e/\rho-f_\eta^2)=0 \tag{16b}$$

$$2V\theta_\eta-\left(\frac{\ell}{Pr}\theta_\eta\right)_\eta-\dot{M}^2R_Df_1(\bar{Y}_i,\theta)/f_2(\theta_w)=0 \tag{16c}$$

$$2V\bar{Y}_{i\eta}-\left(\frac{\ell}{Pr}\bar{Y}_{i\eta}\right)_\eta-\dot{M}^2R_Df_1(\bar{Y}_i,\theta)/f_2(\theta_w)=0 \tag{16d}$$

with the boundary conditions

$$\eta=0: \quad -f=V_w=\dot{m}/2\sqrt{(\rho\mu)_s a}=\dot{M} \tag{17a}$$

$$f_\eta=0 \tag{17b}$$

$$\frac{d\theta}{d\eta}=2\frac{Pr}{\ell}\dot{M}\left[\Delta H_s+\frac{c_{ps}}{c_p}(\theta_w-\theta_u)\right] \tag{17c}$$

$$\frac{d\tilde{Y}_i}{d\eta}=2\frac{Pr}{\ell}\dot{M}\tilde{Y}_{iw} \tag{17d}$$

$$\eta\to\infty: \quad f_\eta=1, \quad \theta=\theta_e, \quad \tilde{Y}_i=\tilde{Y}_{ie}=1 \tag{18}$$

Here it has been assumed that the composition of the approach flow is as specified by the right-hand side of Eq. (8). R_D is the ratio of the homogeneous to the heterogeneous Damköhler number

$$R_D=\bar{K}^{\Sigma\nu_j}p^{\Sigma\nu_j'}\frac{4\exp(-E/RT_r)}{B_s^2T_r^{2m}\exp(-2E_s/RT_r)} \tag{19}$$

The quantity

$$\bar{K}^{\Sigma\nu_j'}=\frac{T_r^{n-\Sigma\nu_j'}}{\rho_s^2}\mu_r B\left(\frac{\bar{M}_r}{R}\right)^{\Sigma\nu_j'}\sum_{j=1}^{N}\nu_j'\bar{M}_j\prod_{j=1}^{N}\left(\frac{Y_j'}{\bar{M}_j}\right)^{\nu_j'} \tag{20}$$

has been introduced by Johnson and Nachbar[9] as $\bar{K}^m=\bar{K}^{-\Sigma\nu_j}$. The functions $f_1(\tilde{Y}_i,\theta)$ and $f_2(\theta_w)$ are given by

$$f_1(\tilde{Y}_i,\theta)=\prod_{j=1}^{N}\left[\frac{\tilde{Y}_j(Y_j''-Y_j')}{Y_j'}+1\right]^{\nu_j'}$$

$$\times\left(\frac{\rho}{\rho_r}\right)^{\Sigma\nu_j'-1}\theta^n\exp\left[-\frac{E}{RT_r}\left(\frac{1}{\theta}-1\right)\right] \tag{21}$$

$$f_2(\theta_w)=\theta_w^{2m}\exp\left[-\frac{2E_s}{RT_r}\left(\frac{1}{\theta_w}-1\right)\right] \tag{22}$$

Equations (16) and the boundary conditions of Eqs. (17) and (18) pose an eigenvalue problem for $\dot{M}$. A closed-form solution is derived for the two limiting cases of frozen and equilibrium flow. The general case is investigated numerically.

Closed-Form Solution

In the following the gas-phase reaction is assumed to be bimolecular,

$$A_1+A_2\to B_1+B_2 \tag{23}$$

with equal molecular weight $\bar{M}_i=\bar{M}$ for all species. Then

$$\tilde{Y}_i(\eta)=\tilde{Y}(\eta) \tag{24}$$

A formal solution is obtained from Eqs. (16) and (17) for the coupling function

$$\vartheta(\eta)=\theta-\tilde{Y}=\frac{2\dot{M}I_ePr/\ell}{1+2\dot{M}I_ePr/\ell}\left[(\theta_e-1)+\frac{c_{ps}}{c_p}(\theta_w-\theta_u)\right.$$

$$\left.+\Delta H_s-\theta_w\right]\frac{I(\eta)-I_e}{I_e}+(\theta_e-1) \tag{25}$$

where

$$I(\eta)=\int_0^\eta\frac{Pr/Pr_w}{\ell/\ell_w}\exp\left(2\int_0^\eta\frac{PrV}{\ell}d\eta\right)d\eta \tag{26}$$

Making use of the boundary conditions given in Eqs. (17c) and (17d), a relation for the nondimensional mass rate of burning is obtained

$$\dot{M}=\frac{(\theta_e-\theta_w)-(1-\tilde{Y}_w)}{2\frac{Pr}{\ell}I_e\left[\frac{c_{ps}}{c_p}(\theta_w-\theta_u)+\Delta H_s-\tilde{Y}_w\right]} \tag{27}$$

which gives the burning rate dependence upon the conditions of the surrounding atmosphere and at the propellant surface. Here the surface concentration $\tilde{Y}_w$ is unknown initially and can be determined only by solving Eqs. (16-18). However, limits of $\tilde{Y}_w$ may be given, which in turn give upper and lower bounds of the burning rate.

Limiting Case

For the two limiting cases of frozen and infinitely fast gas-phase reaction the mass fraction at the propellant surface $\tilde{Y}_w$ may be eliminated from Eq. (27) and one obtains

$$\dot{M}=\frac{\theta_e-\theta_w}{2\frac{Pr}{\ell}I_e\left[\frac{c_{ps}}{c_p}(\theta_w-\theta_u)+\Delta H_s\right]} \tag{28}$$

for frozen flow and

$$\dot{M}=\frac{\theta_e-\theta_w}{2\frac{Pr}{\ell}I_e\left[\frac{c_{ps}}{c_p}(\theta_w-\theta_u)+\Delta H_s-1\right]} \tag{29}$$

for an infinitely fast gas-phase reaction.

These equations give a relation between $\dot{M}$ and θ_w as specified by the transport processes in the flowfield plotted in Fig. 2 for $T_e=705$ K. The integral I_e was computed making use of Eqs. (16a), (16b), and (26), assuming ρ and ℓ to be constant computed at the propellant surface temperature. The relevance of this assumption will be discussed later in this paper. A second dependence is given by the pyrolysis rate law of Eq. (12). This is also plotted in Fig. 2 as a dashed-dotted curve for three different velocity gradients a. The intersections between these sets of curves represent the steady-state solutions. Depending upon the location of the pyrolysis rate curve, either one, two, or three intersections are obtained. Point A represents an ignited state, C denotes a quenched state, and the tangent points Q and I denote the steady-state

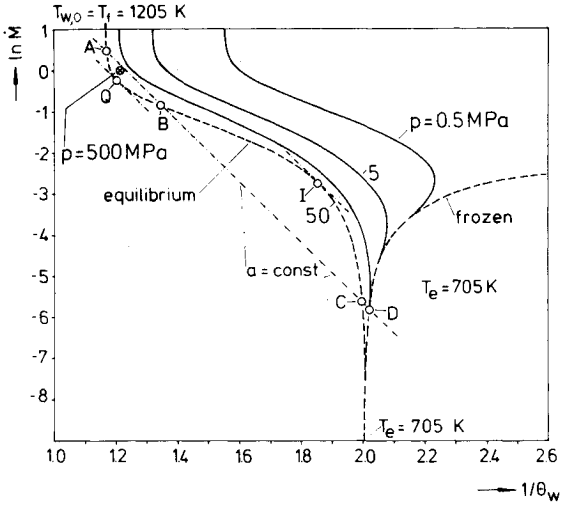

Fig. 2 Dependence of nondimensional burning rate upon surface temperature: closed-form limiting solutions, numerical solution for $p=0.5$, 5, and 50 MPa.

quench and ignition limit. In the frozen-flow case only one solution exists, point D, since the pyrolysis reaction was assumed to be endothermic.

Since to each point of solution there corresponds a value of the velocity gradient a, a dependence of the burning rate $\dot{m}$ upon a is obtained and plotted in Fig. 3. For an infinitely fast gas-phase reaction, which leads to equilibrium gas-phase composition, an S-shaped curve is obtained, characteristic of ignition and quench phenomena. For the frozen flow a monotonous increase of $\dot{m}$ with a is observed. For high values of a both curves merge, i.e., $T_w \to T_e$ for $a \to \infty$ [c.f., Eqs. (28) and (29)].

Numerical Solution and Discussion of Results

A numerical solution of the nonlinear stiff second-order boundary value problem posed by Eqs. (16-18) is obtained by replacing $\bar{Y}$ in Eq. (16c), making use of Eq. (25), and solving Eq. (16c) for $\theta(\eta)$. This was done by employing the shooting procedure based upon the EPISODE package of Byrne and Hindmarsh[8] after introducing an initial assumed value of $\theta(\eta)$ and $\ell(\eta)$ into Eqs. (16a) and (16b). Correcting θ and ℓ with $\theta(\eta)$ and assuming $\ell = \theta^{-0.5}$, an iterative process leads to the final solution of the problem. As will be discussed later, this iteration may be avoided without introducing too large an error if, for ρ and ℓ, values at the propellant surface are used to compute $I(\eta)$. Furthermore $Pr = 0.7$ and $c_{ps}/c_p = 1$ were introduced. Since the velocity component perpendicular to the surface reaches high values, the balance of momentum Eq. (16b) had to be modified to obtain the numerical results. The transformation given by Kubota and Fernandez[12] was used. In this way $\dot{M} = \dot{M}(\theta_w)$ represented in Fig. 4 is obtained for $p = 50$ MPa and various free stream temperature, T_e. The general character of the curves is the same as for the equilibrium case (cf., Fig. 2). Taking into account the pyrolysis rate the burning rate law $\dot{m} = \dot{m}(a)$ is obtained, which is plotted for $p = 50$ MPa and various T_e in Figs. 5 and 6.

It is seen that the burning rate of a monopropellant depends in the entire field of parameters upon the temperature T_e at the edge of the boundary layer and the velocity gradient a, which for a finite body is proportional to the freestream flow velocity U. This dependence is particularly strong in the vicinity of the ignition and quench limits. For low flow velocities the burning rate becomes equal to the rate observed in strand burning experiments b_0 (cf., Ref. 9, Fig. 1). In this case the surface temperature T_w has a definite value T_{w0}, which in this model depends only upon pressure. It lies below the adiabatic flame temperature $T_f = 1205$ K. For high flow velocities the influence of the gas-phase reaction drops out. In this case the burning rate is determined by the rate of pyrolysis and by the heat transfer. The burning rate lies below or above the strand burning value, depending upon whether the free-

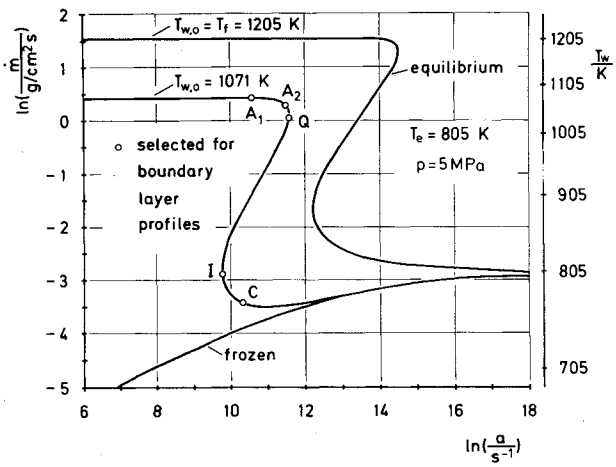

Fig. 3 Dependence of burning rate upon velocity gradient: closed-form limiting solutions, numerical solution for $p = 5$ MPa.

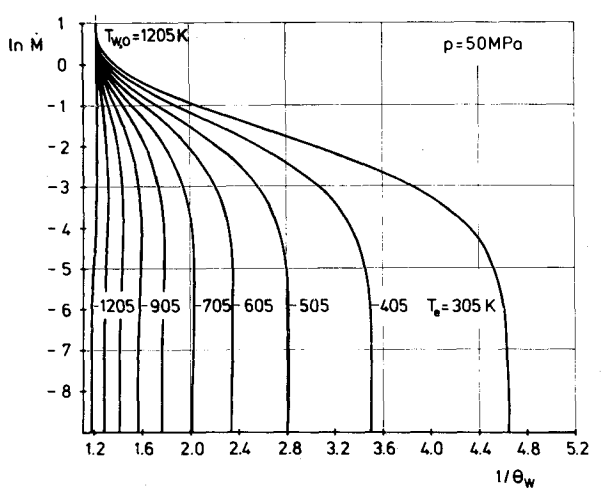

Fig. 4 Nondimensional burning rate vs surface temperature, $p = 50$ MPa.

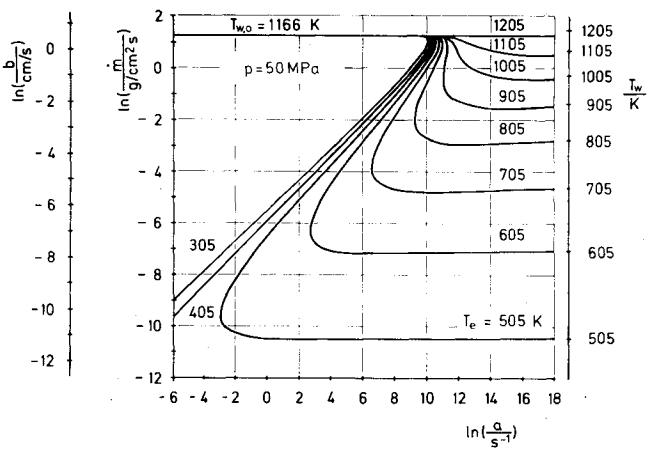

Fig. 5 Burning rate dependence upon velocity gradient (logarithmic representation).

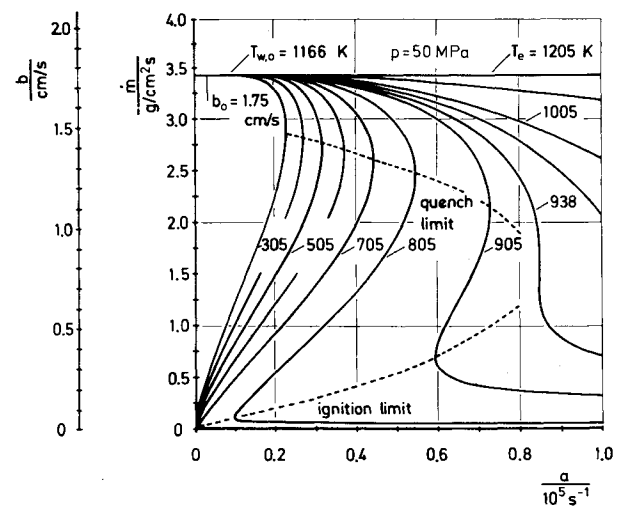

Fig. 6 Burning rate dependence upon velocity gradient.

flow temperature T_e lies below or above the surface temperature T_{w0} when the propellant burns in a gas at rest. Similar behavior has been observed experimentally by Churchill,[3] who found that under high flow rate conditions the propellant frequently decomposed completely without visible ignition.

Except for a free-flow temperature T_e close to the adiabatic flame temperature T_f the burning rate decreases initially with increasing free-flow velocity U, increasing again for larger values of U, when the surface temperature T_w approaches the free flow temperature T_e. If the gas temperature T_e is close to T_f the burning rate increases all the way with increasing flow velocities. However, the gradient of this dependence is rather low.

From these results steady-state ignition and quench limits may also be obtained (see Fig. 6). They show that the surface temperature at which ignition occurs, T_{wi}, depends strongly upon the flow velocity U. Burning rates between ignition and quench limit are unstable. Small disturbances in the velocity gradient result in either the high or low burning rate solution.

All of these results are of particular importance with reference to states and systems where the free-flow temperature differs from the adiabatic flame temperature.

Figure 7 gives a three-dimensional representation of the dependence of $\dot{m}$ upon T_e and a. It is seen that the S-shaped character of this dependence holds with respect to a as well as with respect to T_e, i.,e., ignition and quench phenomena occur when a or T_e are varied.

Boundary-Layer Profiles

The boundary-layer profiles of the nondimensional temperature θ, the fuel species Y_A, the product species Y_B, and the nondimensional homogeneous production rate of species W_B are plotted in Figs. 8-11 for $p=5$ MPa and $T_e=805$ K. In these figures five different states have been selected, indicated by circular points in Fig. 2. They were chosen such that various typical cases are included, Q and I representing states coinciding with the quench and ignition limits, A and C being sufficiently removed from these limits. The temperature profiles drawn in Fig. 8 confirm the conclusions drawn from Figs. 5-7. Case C corresponds to the frozen-flow solution, no homogeneous reaction takes place, and the temperature profile looks like a simple heat flux profile. Decreasing the freestream velocity the ignition state I is reached, as is indicated by the temperature rise at $\eta=0.5$. For the case A_1 the flame is fully developed. After a steep rise close to the propellant surface the temperature has a relatively broad equilibrium profile, being constant over some distance. The temperature profile for case Q shows that in the quench limit the maximum flame temperature has decreased and the equilibrium regime has vanished.

The mass rate of production $W_B(\eta)$ of products B is plotted in Fig. 11 with a stretched boundary-layer coordinate. It is seen that the maximum of the production rate lies directly at the wall in spite of the fact that the temperature maxima are removed from the wall. Apparently the influence of the concentration outweighs the temperature effect. There is, however, a dependence upon pressure, as will be demonstrated.

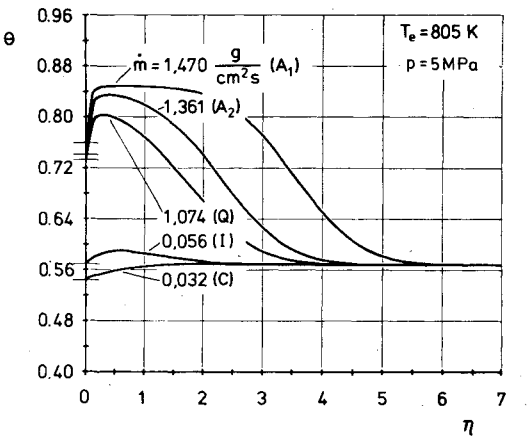

Fig. 8 Boundary-layer profile of temperature.

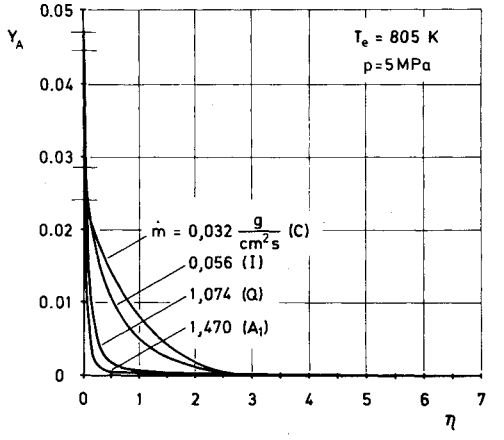

Fig. 9 Reactant mass fraction profile.

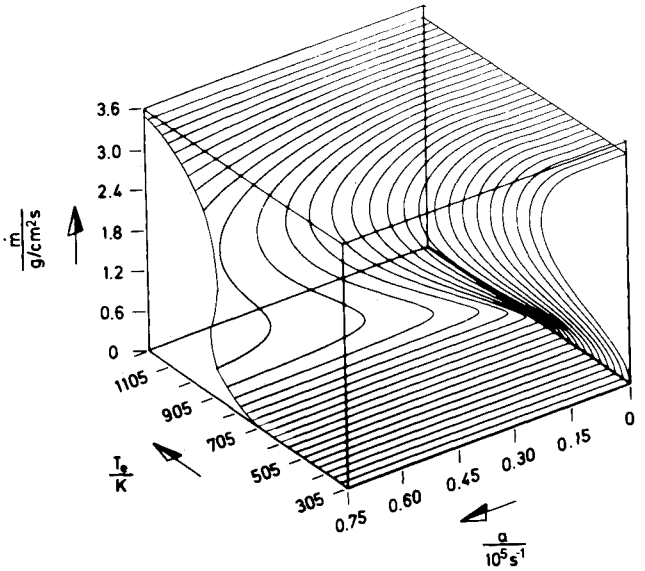

Fig. 7 Three-dimensional representation of data of Fig. 6.

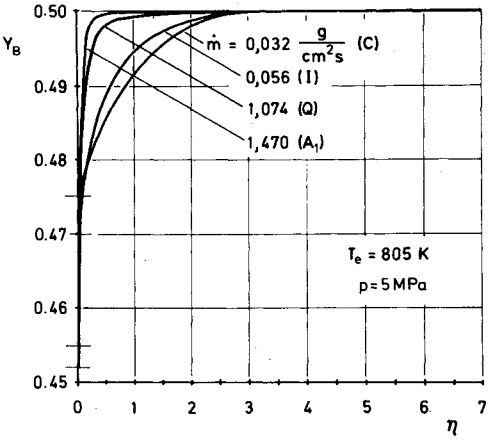

Fig. 10 Profile of product mass fraction ($Y_{B\infty}=0.5$).

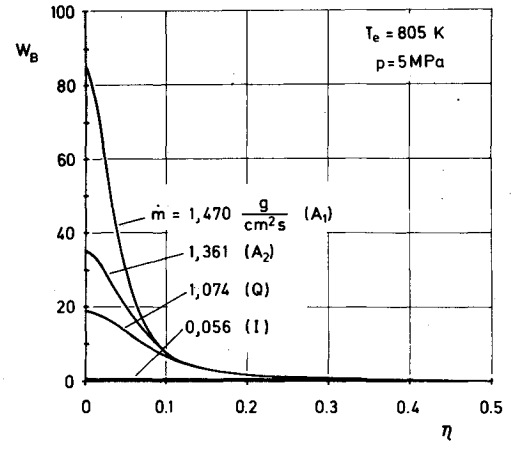

Fig. 11 Boundary-layer profile of rate of gas-phase reaction.

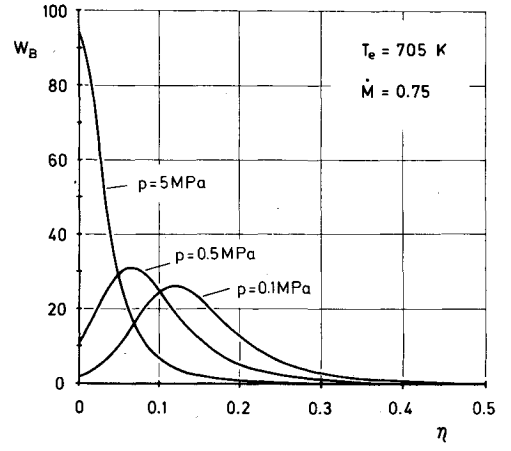

Fig. 13 Boundary-layer profiles of rate of gas-phase reaction for $p = 0.1$, 0.5, and 5 MPa.

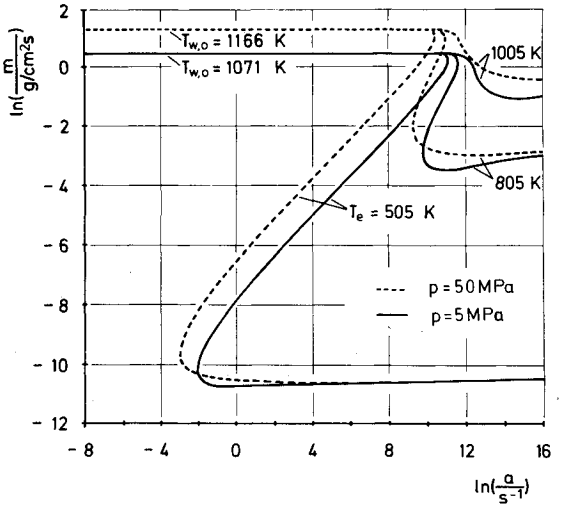

Fig. 12 Burning rate vs velocity gradient for $p = 5$ and 50 MPa.

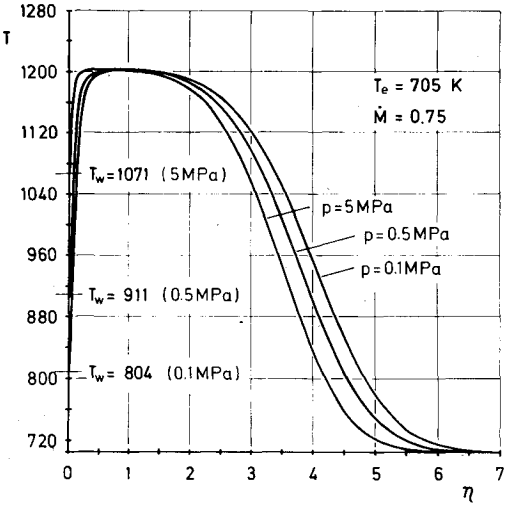

Fig. 14 Temperature profile for $p = 0.1$, 0.5, and 5 MPa.

Influence of Pressure

The influence of pressure is represented in Figs. 2 and 12-14. It is seen in Fig. 12 and particularly in Fig. 2 that with increasing pressure the equilibrium solution is approached. On the other hand, in the quenched state the coincidence with the frozen-flow solution becomes better the smaller the pressure. In this case the burning rate depends upon p as the square root of p. In Fig. 13 the mass rate of production $W_B(\eta)$ has been plotted for three different pressures. It is seen that with decreasing pressures the reaction zone shifts away from the wall. However, at $p = 5$ MPa it still appears to be well attached to it. This behavior is corroborated by the temperature profiles shown in Fig. 14. It has due consequences upon approximate flame theories imposing corresponding matching conditions to the wall region.

Density Iteration

It has been pointed out at the beginning of this section that the numerical procedure is based upon an iteration process as far as the determination of the integral function $I(\eta)$ is concerned. It turned out, however, that this may be avoided if in Eqs. (16a) and (16b) values at the propellant surface are used for ρ and ℓ. This result is demonstrated in Fig. 15 where $\ell n\dot{M}$ is plotted vs $1/\theta_w$ for two freestream flow temperatures. It is seen that the values obtained by iteration coincide closely with the results obtained with $\rho = \rho_w$ and $\ell = \ell_w$, whereas the results obtained with $\rho = \rho_e$ and $\ell = 1$ differ noticeably at lower values of T_e.

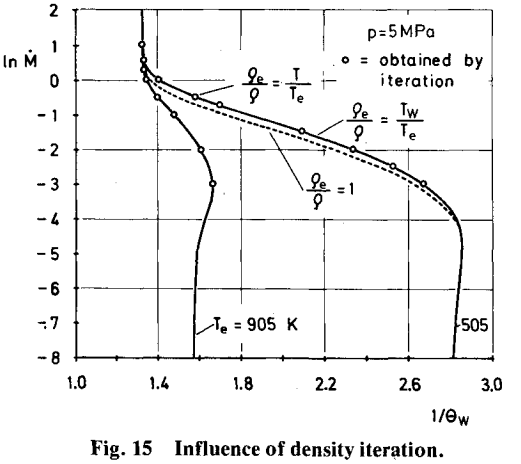

Fig. 15 Influence of density iteration.

Conclusions

In the entire field of parameters the burning rate $\dot{m}$ of a monopropellant depends upon the velocity and the temperature of the freestream flow. This dependence is strong in the vicinity of the ignition and quench limits.

For low flow velocities the burning rate becomes equal to the strand burning value with a surface temperature T_{w0} below the adiabatic flame temperature. For high flow

velocities the influence of the gas-phase reaction drops out and the surface temperature approaches asymptotically the free-flow temperature. Then the burning rate is determined by heat transfer and pyrolysis only. This burning rate lies below or above the strand burning value if $T_e < T_{w0}$ or $T_e > T_{w0}$.

Except for a free-flow temperature close to the adiabatic flame temperature the rate of burning decreases initially with increasing free-flow velocity U, increasing again for higher values of U. If the temperature T_e is close to the adiabatic flame temperature, $\dot{m}$ increases slowly all the way with increasing U. The steady-state ignition and quench limits obtained show that the surface temperature T_{wi} at which ignition occurs depends strongly upon the flow velocity.

All of these results have a particular importance with reference to those states and systems where the freestream temperature differs considerably from the adiabatic flame temperature.

For the limiting cases of frozen flow and for very fast gas-phase reaction a solution was derived in closed form. Comparison with the numerical solution shows that the limiting case of fast gas-phase reaction is approached with increasing pressure, whereas the frozen-flow limit is approached with increasing flow velocity or decreasing pressure.

References

[1] Mukunda, H. S., "A Comprehensive Theory of Erosive Burning in Solid Rocket Propellants," *Combustion, Science and Technology*, Vol. 18, 1978, pp. 105-118.

[2] Razdan, M. K. and Kuo, K. K., "Erosive Burning Study of Composite Solid Propellants by Turbulent Boundary-Layer Approach," *AIAA Journal*, Vol. 17, Nov. 1979, pp. 1225-1233.

[3] Churchill, S. W., Kruggel, R. W., and Bier, J. C., "Ignition of Solid Propellants by Forced Convection," *AIChE Journal*, Vol. 2, 1956, pp. 568-571.

[4] Birk, A. and Cavenuy, L. H., "Convective Ignition of Propellant Cylinders," *AIAA Journal*, Vol. 18, Nov. 1980, pp. 1363-1370.

[5] Tsuji, H., "An Aerothermochemical Analysis of Erosive Burning of Solid Propellant," *9th Symposium (International) on Combustion*, Academic Press, New York, 1963, pp. 384-393.

[6] Schuyler, F. L. and Torda, T. P., "An Aerothermochemical Analysis of Solid Propellant Combustion," *AIAA Journal*, Vol. 4, Dec. 1966, pp. 2171-2177.

[7] Kuo, K. K. and Summerfield, M., "High Speed Combustion of Mobile Granular Solid Propellants: Wave Structure and the Equivalent Rankine-Hugoniot Relation," *15th Symposium (International) on Combustion*, The Combustion Institute, Pittsburgh, Pa., 1975, pp. 515-527.

[8] Byrne, G. D. and Hindmarsh, A. C., "A Polyalgorithm for the Numerical Solution of Ordinary Differential Equations," *ACM Transactions of Mathematical Software*, Vol. 1, 1975, pp. 71-96.

[9] Johnson, W. F. and Nachbar, W., "Deflagration Limits in the Steady Linear Burning of a Monopropellant with Application to Ammonium Perchlorate," *8th Symposium (International) on Combustion*, Williams & Wilkins Co., Baltimore, Md., 1962, pp. 678-689.

[10] Chung, P. M., "Chemically Reacting Nonequilibrium Boundary Layers," *Advances in Heat Transfer*, Vol. 2, edited by J. P. Harnett and T. F. Irvine, Academic Press, New York, 1965, pp. 110-271.

[11] Adomeit, G., Mohiuddin, G., and Peters, N., "Boundary-Layer Combustion of Carbon," *16th Symposium (International) on Combustion*, Academic Press, New York, 1976, pp. 731-743.

[12] Kubota, T. and Fernandez, F. L., "Boundary Layer Flow with Large Injection and Heat Transfer," *AIAA Journal*, Vol. 6, Jan. 1968, pp. 22-28.